# Supporting information:

# Evolving a polymerase for hydrophobic base analogues

D. Loakes, J. Gallego, V.B. Pinheiro, E.T. Kool and P. Holliger

## 1. Figure legends

**Supporting information Figure 1 (see pages S2-S3):**

**Alignment of polymerase sequences**: Protein sequences of selected polymerases from round 4 (4C11) and round 5 (5B1, 5B4, 5D3, 5D4) are aligned with parent polymerases Taq, Tth and Tfl. Numbering here refers to the Tth gene, which contains two insertions (59G, 228E) compared to the Taq and Tfl genes, i.e. in Taq (and Tfl), which do not share the Tth insertions G59 and E228, actual residue numbers (N) will be N=n—1 (for n>58), respectively N=n-2 (for n>228). Identities are outlined and background is shaded dark grey. Substitutions are outlined with a white background (for non-conservative substitutions (e.g. R -> E)) or light grey background (for conservative substitutions (e.g. R -> K)).

A number of mutations that are not present in the parental genes but are shared by several selected polymerases are shown in Supporting information Table 1

# Alignment of polymerase sequences

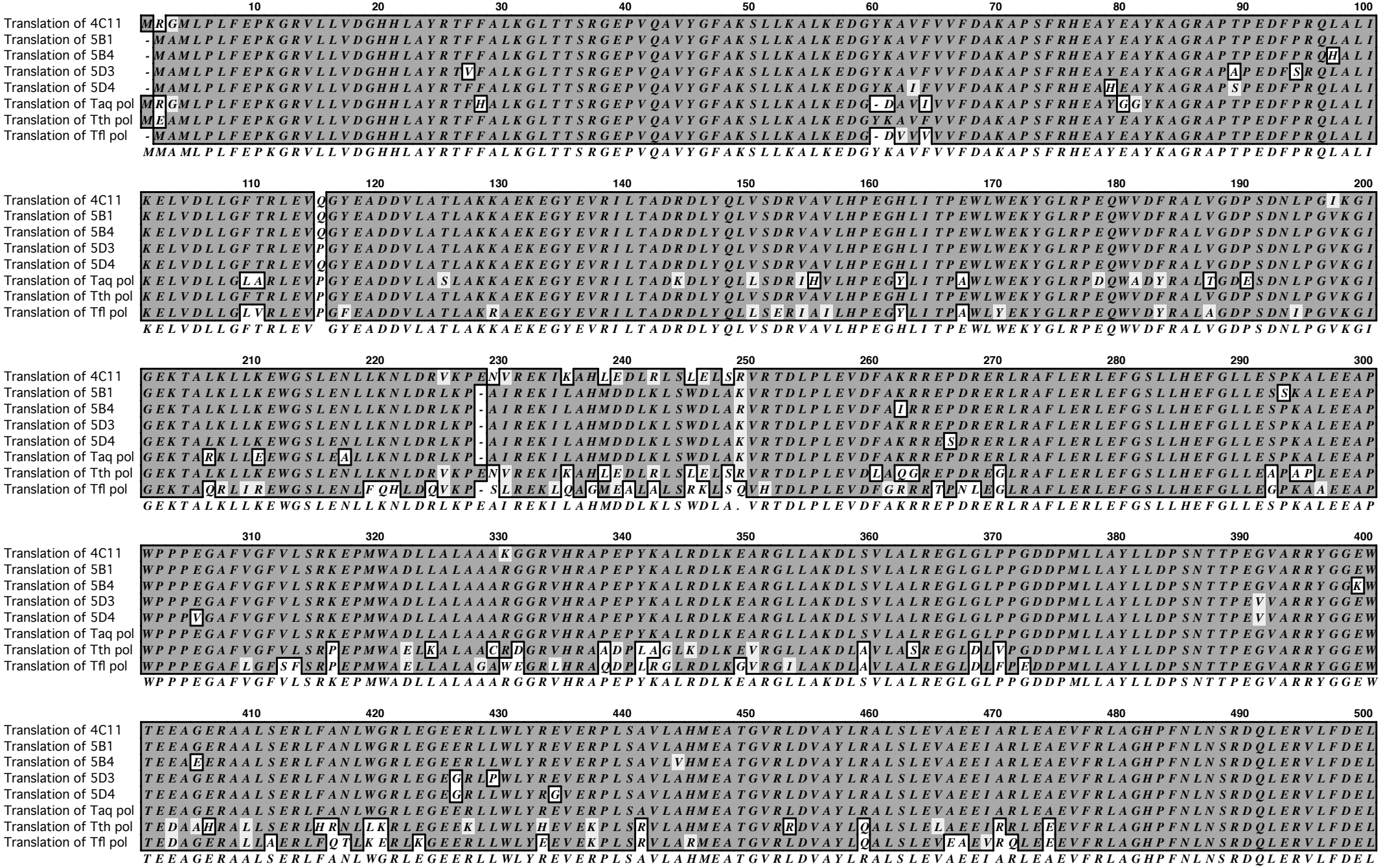

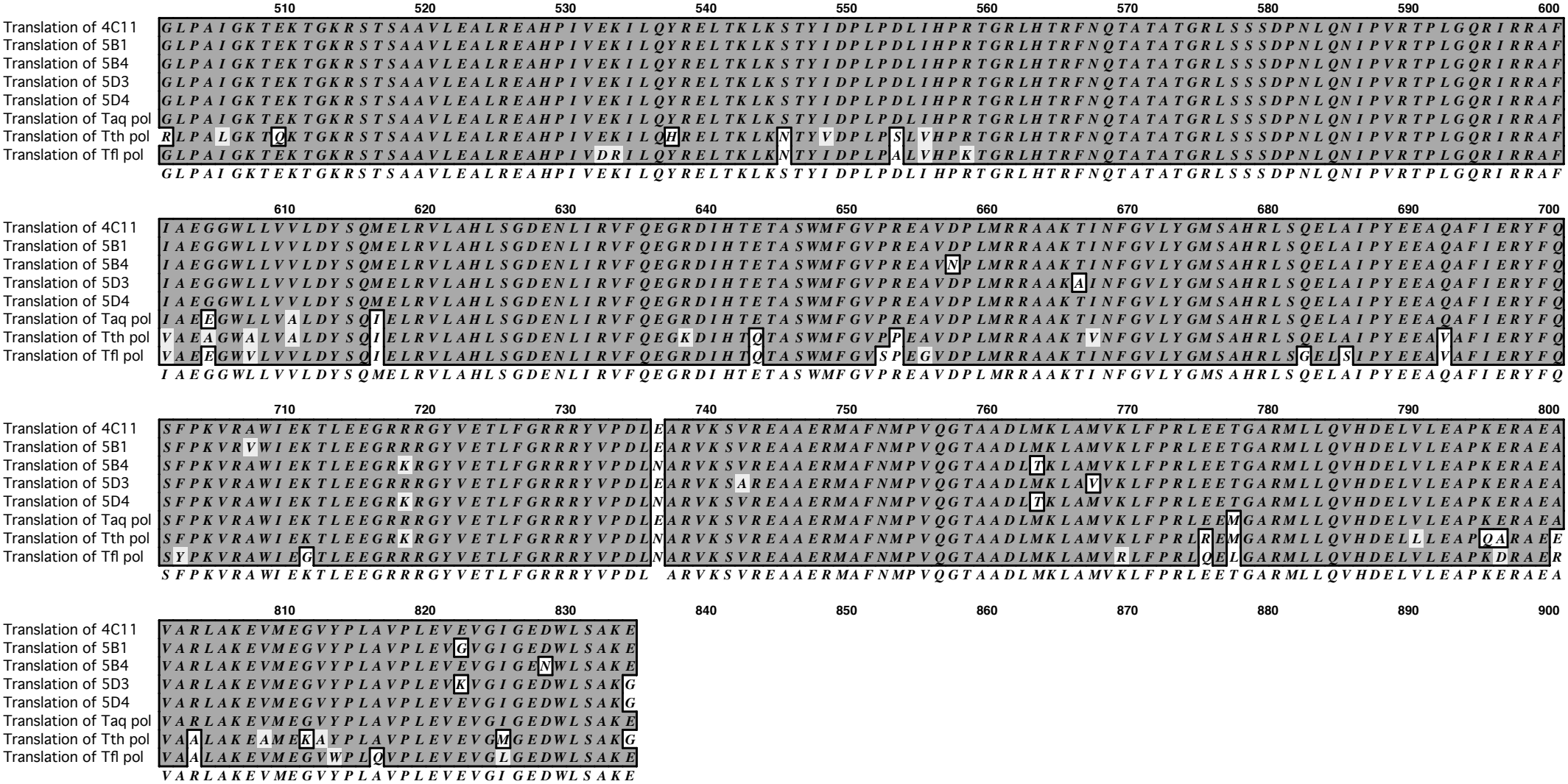


Supporting information Fig. 1: Alignment of polymerase sequences

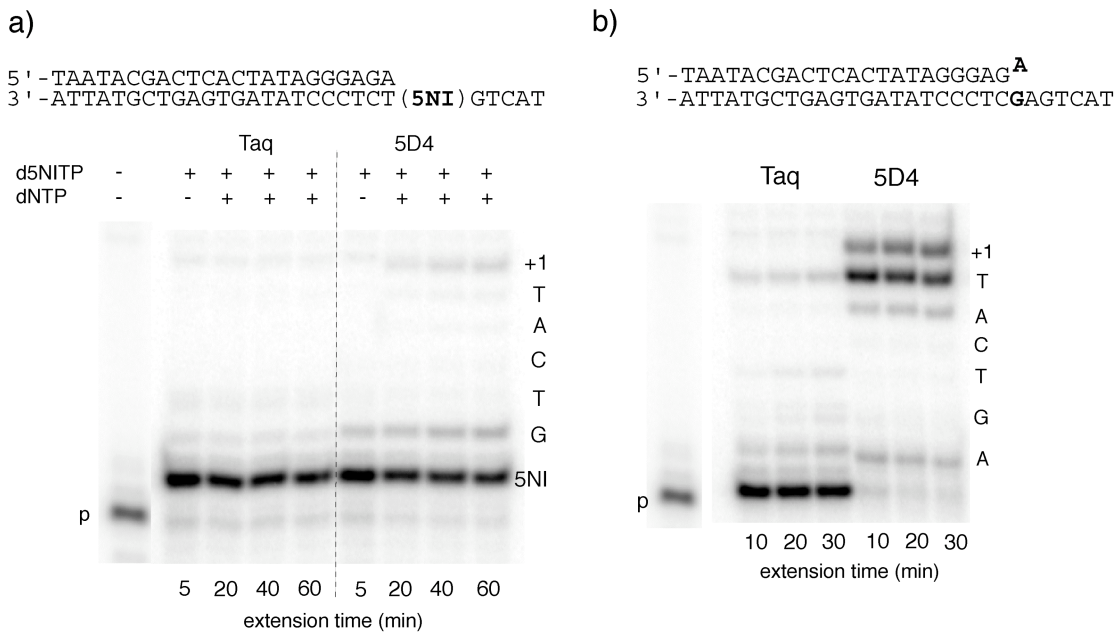


**Supporting information Figure 2: Formation and extension of the d5NI self-pair and transversion mismatch extension.**

(a) Formation and extension of a d5NI-d5NI self-pair is shown for both Taq and 5D4. While d5NI-TP is incorporated efficiently opposite template d5NI by both polymerases, further extension of the self-pair is stalled in both cases, with only 5D4 showing some weak extension (< 5%). (b) Primer extension (%) is plotted against time for extension of an A·G mismatch by both Taq and 5D4. While Taq is unable to extend the mismatch, it is efficiently extended by 5D4.

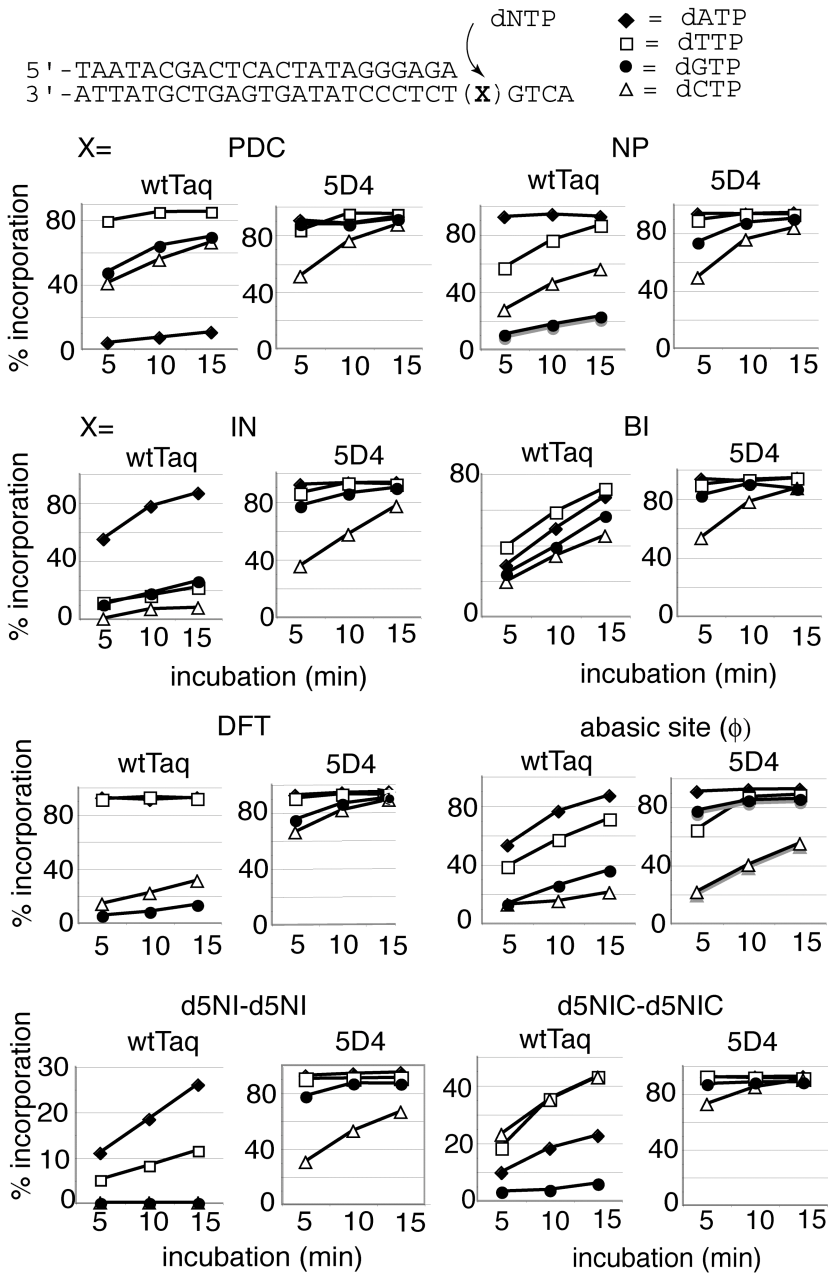


**Supporting information Figure 3: Incorporation specificity opposite HBAs.** Primer extension (%) is plotted against time for incorporation of dATP (black diamonds), dTTP (open squares), dGTP (filled circles), dCTP (open triangles) for unnatural template bases NP, PDC, DFT, I, BI, $[d5NI]_2$ (2 consecutive d5NI bases), $[d5NIC]_2$ (2 consecutive d5NIC bases) and an abasic site (tetrahydrofuran (ϕ)) by polymerases Taq and 5D4. 5D4 displays greatly reduced incorporation bias for several HBA template bases with some (NP, PDC, DFT) approaching universal base behaviour.

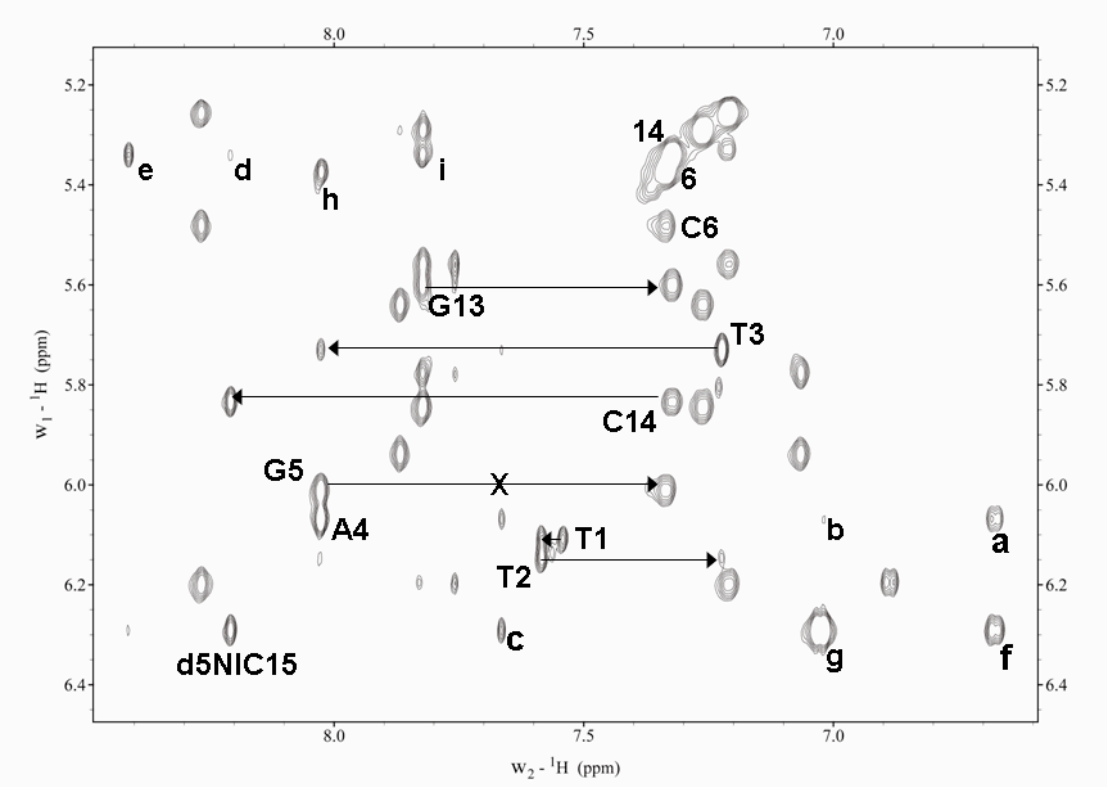


**Supporting information Figure 4: NMR.**

Aromatic–H1' region of the $D_2O$ NOESY spectra (250 ms mixing time) of *tnic*, recorded at 25°C. Intra-residue pyrimidine H6-H1' and purine/d5NIC H8–H1' cross-peaks are labelled with residue name and number, intra-residue pyrimidine H5-H6 cross-peaks are labelled with residue number, and sequential NOE connectivities are indicated with arrows. For clarity, only T1 to C6 and G13 to d5NIC15 assignments are shown. Cross-peaks (a) to (i) are assigned as follows: (a) d5NIC15 H2-A4 H1'; (b) d5NIC15 H3-A4 H1'; (c) A4 H2-d5NIC15 H1'; (d) d5NIC15 H8-C14 H5; (e) d5NI15 H6-C14 H5; (f) d5NIC15 intra-residue H2-H1'; (g) d5NIC15 intra-residue H3-H1'; (h) G5 H8-C6 H5; (i) G13 H8-C14 H5. The absence of the sequential A4 H2-G5 H1' NOE is marked with an "X".

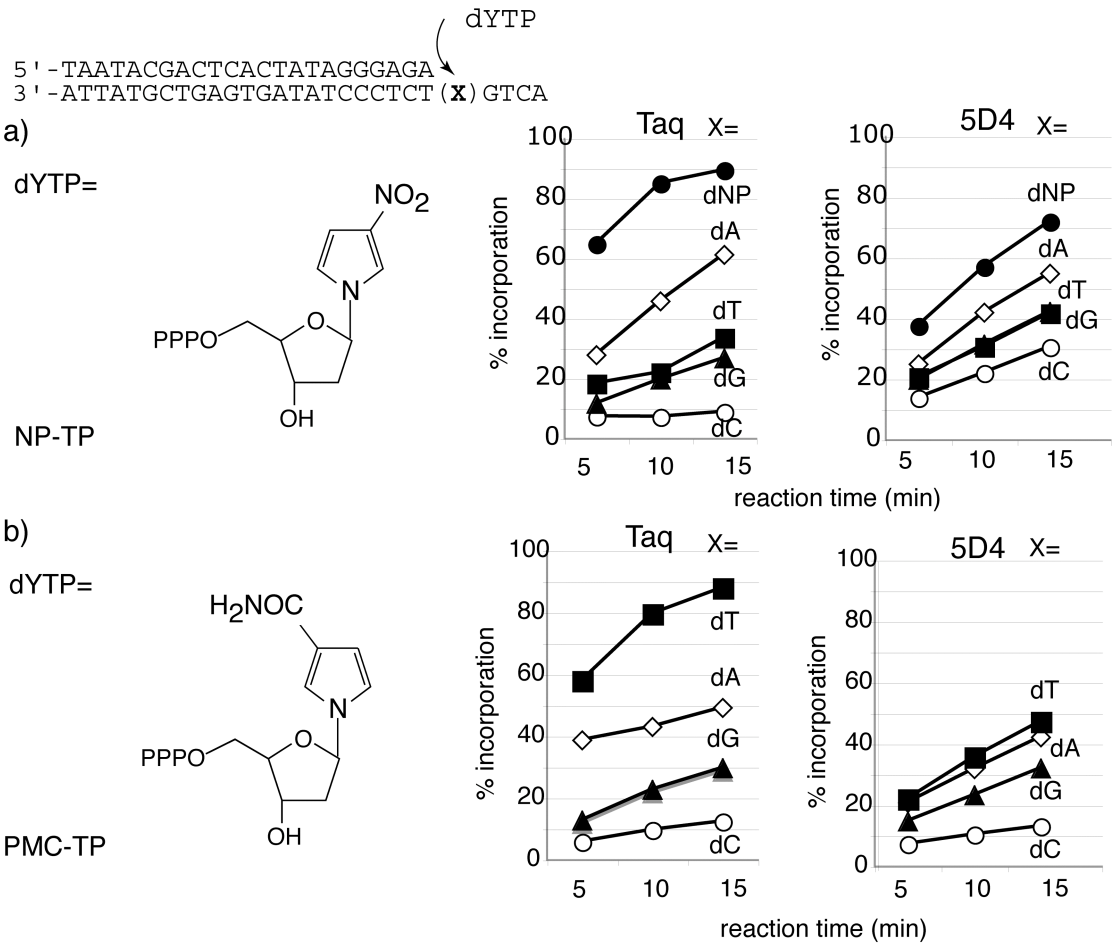


**Supporting information Figure 5: Incorporation of HBA triphosphates.** Nucleotide triphosphate incorporation (%) is plotted against time for incorporation of dYTP (a) Nitro-pyrrol-triphosphate (NP-TP) and (b) Pyrrol-monocarboxamide-triphosphate (PMC-TP) for template X=dA (open diamonds), dT (filled squares), dG (filled triangles), dC (open circles) and dNP (filled circles (a)) for both Taq and 5D4. Incorporation efficiencies are comparable with Taq slightly superior.

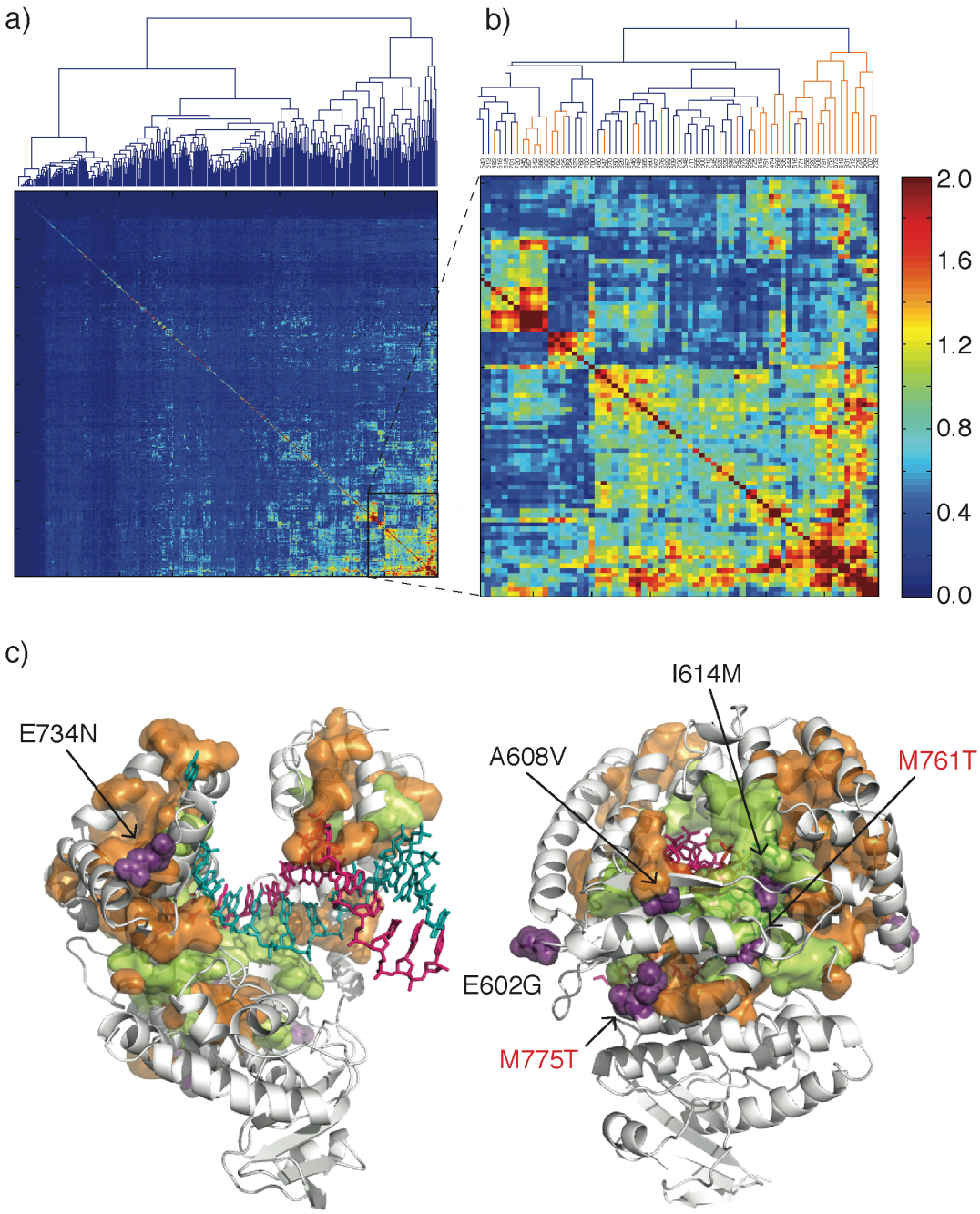


**Supporting information Figure 6: SCA.** Statistical coupling analysis (SCA)[1] of bacterial polymerases. The hierarchical clustering of the output coupling matrix (a) and a detail of the region containing the highest coupling values (b) are shown. Residues with couplings above $\Delta\Delta G = 1.8\ kT^*$ were selected to represent the SCA network, mapped to the structure of the Taq polymerase domain (3KTQ[2]) shown coloured orange in surface representation (c). Conserved residues (> 97% identity) are shown as the green surface. The template strand is shown in teal and primer strand in magenta. 5D4 mutations are shown in purple. Mutations M761T and M775T with connections to the SCA network are labelled in red.

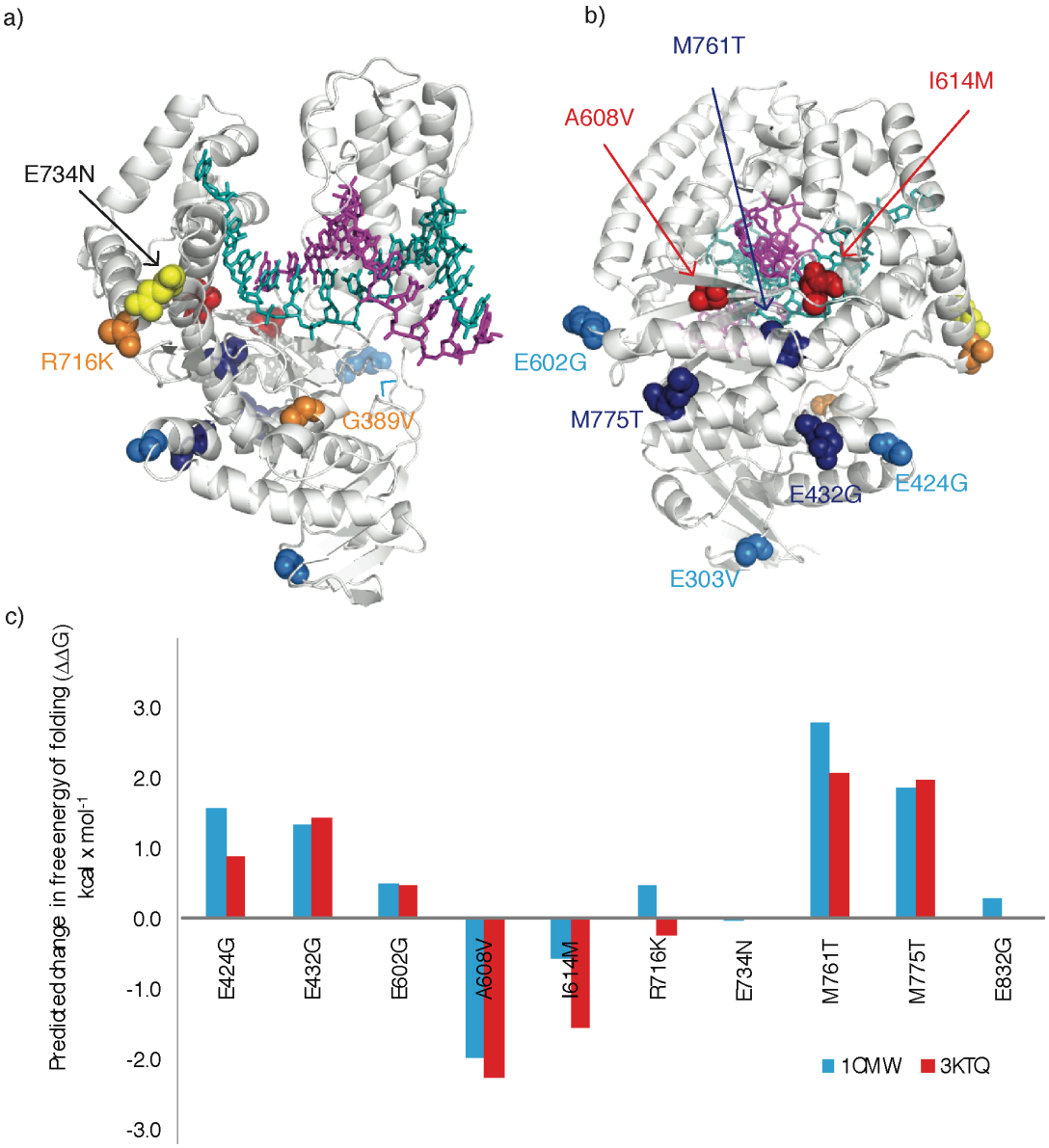


**Supporting information Figure 7: FoldX analysis of 5D4 mutations.** FoldX was used to predict the change in free energy of folding due to individual point mutations in the available Taq structures (see supporting information Table 5). Predictions were ranked and mutations are shown superimposed on the Taq structure (3KTQ) (a, b) and coloured according to their effect on ΔΔG: red = stabilising mutations (ΔΔG < -1.0 kcal mol$^{-1}$ in most structures, e.g. A608V, I614M), orange = weakly stabilising mutations (-1.0 < ΔΔG < 0.0 kcal mol$^{-1}$, e.g. R715K, G389V), yellow = neutral mutations (e.g. E734N), light blue = potentially destabilising (0.0 < ΔΔG < 1.0 kcal mol$^{-1}$, e.g. E602G, E424G) and dark blue = destabilising mutations (ΔΔG > 1.0 kcal mol$^{-1}$, e.g. M761T, M775T). (c) Predicted change in free energy of folding (ΔΔG) in kcal mol$^{-1}$ is plotted for individual mutations for two different Taq structures 1CMV[3] (Apoform) and 3KTQ[2] (closed ternary complex).

a)

1:5'-CAGGAAACAGCTATGACAAAAATCTAGATAACGAGGGCAA
4:5'-GTAAAACGACGGCCAGTACCACGGAACTGCGGGTGACGCCAAGCG

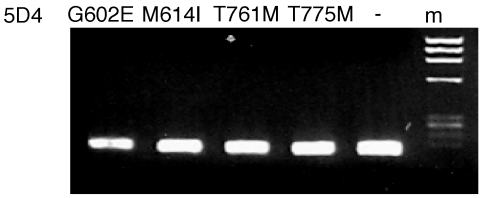


b)

2:5'-CAGGAAACAGCTATGACAAAAATCTAGATAACGAGGGCA(**X**)
6:5'-GTAAAACGACGGCCAGTACCAC(**X**)GAACTGCGGGTGACGCCAAGC(**X**)

**X**= d5NIC

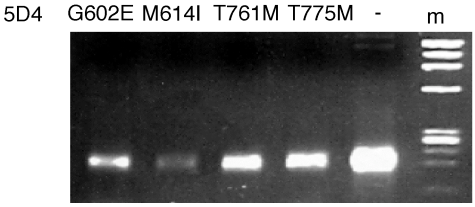


**Supporting information Figure 8: d5NIC PCR of reversion mutants.**

PCR amplification using (a) unmodified standard primers (1,4), or primers in which either only the 3' terminal base (2) or the 3' terminal base as well as an internal base are substituted by d5NIC (6) for reversion mutants (from left to right) (5D4:G602E, 5D4:M614I, 5D4:T761M, 5D4:T775M) as well as 5D4. While all polymerases show comparable activity with unmodified primers only 5D4:M614I shows a significant relative reduction in PCR activity with d5NIC-modified primers. m, ϕX174 HaeIII digest marker.

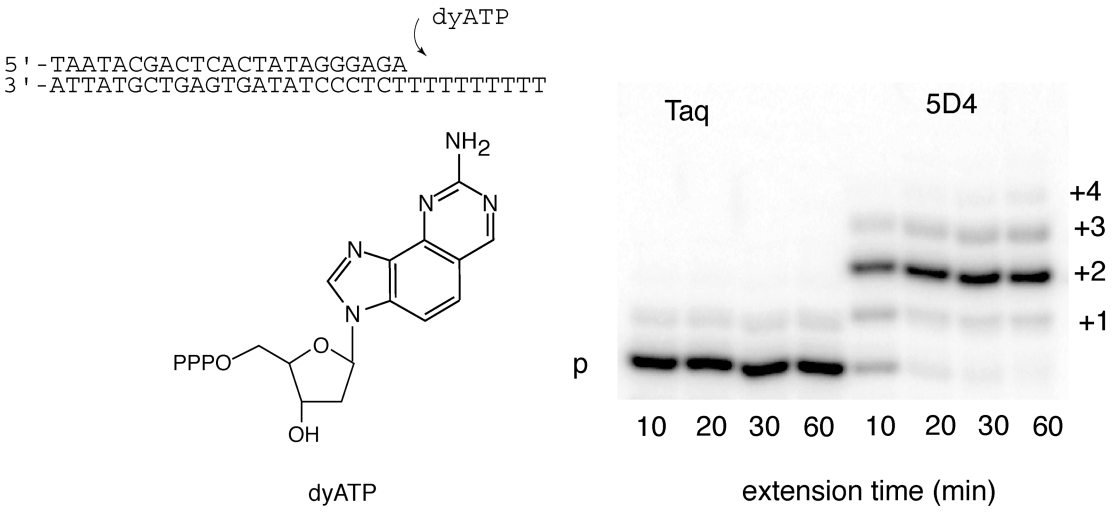


**Supporting information Figure 9: Incorporation of dyATP**

Incorporation of the size-expanded dATP analogue dyATP[4] is shown for both Taq and 5D4. While incorporation by Taq is poor and stalls at +1, 5D4 can incorporate up to +4.

## 2. Supporting Tables

**Supporting Table 1: Shared point mutations in the polymerase domain** (numbering of mutations refers to the Taq gene).

| Mutations[a] | 4C11 | 5B1 | 5B4 | 5D3 | 5D4 |
|---|---|---|---|---|---|
| E602G | + | + | + | + | + |
| A608V | + | + | + | + | + |
| I614M | + | + | + | + | + |
| M762T | | | + | | + |
| M775T | + | + | + | + | + |

**Supporting Table 2: $K_m$ ($\mu$M) and $k_{cat}/K_m$ values ($\%min^{-1}\mu M^{-1}$) for Taq and 5D4 (Fig. 2a)**

| dXTP | Template base | $K_m$ wtTaq | $k_{cat}/K_m$ wt*Taq* | $K_m$ 5D4 | $k_{cat}/K_m$ 5D4 | *f* |
|---|---|---|---|---|---|---|
| 5NI | dA | 111 | 2.8 | 9 | 227.6 | 81 |
| | dT | 109 | 1.5 | 8 | 316.1 | 211 |
| | dC | 26 | 2.0 | 3 | 1364.4 | 682 |
| | dG | 34 | 2.1 | 5 | 683.9 | 326 |
| | | | | | | |
| 5NIC | dA | 13 | 29.6 | 3 | 1475.9 | 50 |
| | dT | 10 | 42.4 | 5 | 529.9 | 13 |
| | dC | 9 | 15.6 | 2 | 796.6 | 51 |
| | dG | 15 | 19.3 | 1 | 2103.4 | 109 |
| | | | | | | |
| A | d5NI | 76 | 0.3 | 28 | 21.4 | 71 |
| T | | 51 | 0.5 | 38 | 11.8 | 24 |
| C | | 11 | 0.10 | 14 | 5.3 | 53 |
| G | | 20 | 0.07 | 28 | 5.3 | 76 |
| NI | | 8 | 9.2 | 9 | 314.9 | 34 |
| | | | | | | |
| A | d5NIC | 27 | 0.2 | 41 | 13.4 | 67 |
| T | | 55 | 0.1 | 33 | 13.6 | 136 |
| C | | 47 | 0.1 | 93 | 2.2 | 22 |
| G | | 99 | 0.04 | 145 | 4.4 | 109 |
| NIC | | 9 | 3.2 | 1 | 979.3 | 306 |
| | | | | | | |
| T | dA | 3 | 187.6 | 3 | 498.9 | 2.7 |
| G | dC | 3 | 763.0 | 2 | 1069.0 | 1.4 |

Relative catalytic efficiency: $f = k_{cat}/K_m$ 5D4 / $k_{cat}/K_m$ wtTaq

**Supporting Table 3: Steady-state extension constants $k_{cat}$ of 3' d5NI by 5D4 (%$min^{-1}\mu M^{-1}$)**

| 3' base | Template N | template N+1 | $k_{cat}/K_m$ |
|---|---|---|---|
| d5NI | A | A | 3.0 |
| | A | T | 2.6 |
| | C | A | 4.6 |
| | C | T | 3.7 |
| | C | C | 4.4 |
| | | | |
| d5NIC | T | A | 40.3 |
| | T | T | 10.3 |

**Supporting Table 4 NMR.**
Experimental constraints and refinement analysis for the *tni* and *tnic* NMR model structures

| **Experimental constraints**[1] | ***tni*** | ***tnic*** |
|---|---|---|
| NOE distance constraints | 228 | 236 |
| Hydrogen bonding distance constraints | 6 | 8 |
| Dihedral constraints | 50 | 48 |
| **Refinement Analysis** | ***tni*** | ***tnic*** |
| Distance constraint violation energy[2] (kcal $mol^{-1}$) | 6.9 | 3.3 |
| Dihedral constraint violation energy[3] (kcal $mol^{-1}$) | 14.2 | 12.4 |
| rms deviation from ideal bond lengths (Å) | 0.02 | 0.02 |
| rms deviation from ideal bond angles (°) | 1.9 | 1.8 |

[1]for residues T1-C6 and G13-d5NI(C)15 (see Methodology)

[2]Force constant K = 50 Kcal $mol^{-1}$ $Å^{-2}$

[3]Force constant K = 0.01 Kcal $mol^{-1}$ $deg^{-2}$

**Supporting Table 5:** FoldX calculation of ΔΔG changes of polymerase domain mutations for different structures of Taq polymerase

| Mutation | Structure | | | | |
|---|---|---|---|---|---|
| | 1CMW | 1KTQ | 4KTQ | 2KTQ | 3KTQ |
| P264S | 0.91 | N.S. | N.S. | N.S. | N.S. |
| E303V | 0.10 | 0.40 | 0.19 | 0.74 | 0.56 |
| G389V | 0.72 | -1.19 | -0.38 | -0.71 | 0.12 |
| E424G | 1.57 | 0.03 | -0.18 | 0.54 | 0.88 |
| E432G | 1.34 | 1.67 | 0.22 | 1.73 | 1.42 |
| E602G | 0.5 | 0.57 | -0.04 | 0.84 | 0.47 |
| A608V | -1.98 | -2.79 | -2.35 | 0.10 | -2.27 |
| I614M | -0.56 | -0.52 | -0.86 | -1.10 | -1.54 |
| R716K | 0.48 | -0.55 | -0.2 | -0.41 | -0.23 |
| E734N | -0.03 | 0.19 | 0.08 | 0.26 | 0.00 |
| M761T | 2.79 | 2.45 | 1.84 | 2.30 | 2.07 |
| M775T | 1.85 | 1.47 | 0.91 | 2.33 | 1.98 |
| E832G | 0.28 | N.S. | N.S. | N.S. | N.S. |

Changes in the predicted free energy of folding (ΔΔG) of Taq polymerase domain point mutants. FoldX was used to predict the effect on protein stability for each individual 5D4 mutation using some of the different Taq polymerase domain structures available. Mutations are numbered as per 1CMW structure. Structures used included apo structures for the full length Taq (1CMW[3]) and Klentaq fragment (1KTQ[2]), the binary complex of polymerase bound to DNA (4KTQ[2]), and both open (2KTQ[2]) and closed (3KTQ[2]) ternary complexes of Taq polymerase with DNA and incoming nucleotide. Energy is given as kcal $mol^{-1}$. Residues not present in the structure are shown as N.S. .

## 3. List of primers (X=d5NIC, Y=d5NI)

1: 5’-CAG GAA ACA GCT ATG ACA AAA ATC TAG ATA ACG AGG GCA **X**-3’

2: 5’- GTA AAA CGA CGG CCA GTA CCA CCG AAC TGC GGG TGA CGC CAA GC**X** -3’

3: 5’-CAG GAA ACA GCT ATG ACA AAA ATC TAG ATA **X**CG AGG GCA **X**-3’

4: 5’-GTA AAA CGA CGG CCA GTA CCA C**X**G AAC TGC GGG TGA CGC CAA GC**X**-3’

5: 5’-GTA AAA CGA CGG CCA GTA C**X**A CCG AAC TGC GGG TGA CGC CAA G**X**-3’

6: 5’-CAG GAA ACA GCT ATG ACA AAA ATC TAG ATA **Y**CG AGG GCA **Y**-3’

7: 5’-GTA AAA CGA CGG CCA GTA CCA C**Y**G AAC TGC GGG TGA CGC CAA GC**Y**-3’

8-10: primers 1-3 as described[5]

11-13: primer 1, 2, 5 as described[6]

14: 5’-CAG GAA ACA GCT ATG ACA AA-3’

15: 5’-GTA AAA CGA CGG CCA GTA CC-3’

16-19: 5’-AGC TAC CAT GCC TGC ACG CAG C**N**G GCA TCC GTC GCG ACC ACG TT**B** TTC GTG GTC GCG ACG GAT GCC **X**-3’
**N=dA, dG, dC, dT; B=dU-biotin**

20-23: 5’-AGC TAC CAT GCC TGC ACG CAG C**N**G GCA TCC GTC GCG ACC ACG TT**B** TTC GTG GTC GCG ACG GAT GCC **Y**-3’
**N=dA, dG, dC, dT; B=dU-biotin**

20. 5'-TAA TAC GAC TCA CTA TAG GGA GA-3’

21. 5'-TAA TAC GAC TCA CTA TAG GGA GA**X**-3’

22. 5'-TAA TAC GAC TCA CTA TAG GGA GA**Y**-3’

23. 5’- ACTG**X**T CTC CCT ATA GTG AGT CGT ATT A-3’

24. 5’- ACTG**Y**T CTC CCT ATA GTG AGT CGT ATT A-3’

25. 5’- ACTG**Z**T CTC CCT ATA GTG AGT CGT ATT A-3’
**Z = DPC, NP, DFT, abasic site (ϕ), IN, BI, ICS, 7AI**

26. 5’-TAG CTA **X**TC TCC CTA TAG TGA GTC GTA TTA-3’

27. 5’-TAG CTA **Y**TC TCC CTA TAG TGA GTC GTA TTA-3’

28. 5'-TAA TAC GAC TCA CTA TAG GGA GA**Z**-3’
**Z = ICS, 7AI**

29. 5’-**NN**T CTC CCT ATA GTG AGT CGT ATT A-3’
**N = dA, dT, dC, dG**

30. 5’-TTT TTT TTT T**Z**T CTC CCT ATA GTG AGT CGT ATT A-3’
**Z** = **abasic site (ϕ)**

31: 5’-ACC GCC GCC GAC CTC ATG AAG CTG GCT ATG GTG A-3’

32: 5’-TCA CCA TAG CCA GCT TCA TGA GGT CGG CGG CGG T-3’

33: 5’-GGC CTT CAT CGC CGA GGA GGG GTG GCT ATT GGT GG-3’

34: 5’-CCA CCA ATA GCC ACC CCT CCT CGG CGA TGA AGG CC-3’

35: 5’-GGT CCT GGA CTA TAG TCA GAT CGA GCT CAG GGT GCT G-3’

36: 5’-CAG CAC CCT GAG CTC GAT CTG ACT ATA GTC CAG GAC C-3’

37: 5’-CCC CAG GCT GGA GGA AAT GGG CGC CAG GAT GCT CCT TCA G-3’

38: 5’-CTG AAG GAG CAT CCT GGC GCC CAT TTC CTC CAG CCT GGG G-3’

39: 5’-ACC CGC CTC GAG GTC CCA GGC TAC GAG GCG GAC-3’

40: 5’-GTC CGC CTC GTA GCC TGG GAC CTC GAG GCG GGT-3’

## References


1. Lockless, S. W.; Ranganathan, R., *Science* **1999,** *286*, 295-299.
2. Li, Y.; Korolev, S.; Waksman, G., *EMBO J.* **1998,** *17*, 7514-7525.
3. Urs, U. K.; Murali, R.; Krishna Murthy, H. M., *Acta Crystallogr D Biol Crystallogr* **1999,** *55*, 1971-1977.
4. Lu, H.; He, K.; Kool, E. T., *Angew. Chem. Int. Ed.* **2004,** *43*, 5834-5836.
5. d'Abbadie, M.; Hofreiter, M.; Vaisman, A.; Loakes, D.; Gasparutto, D.; Cadet, J.; Woodgate, R.; Paabo, S.; Holliger, P., *Nat Biotechnol* **2007,** *25*, 939-943.
6. Ghadessy, F. J.; Ong, J. L.; Holliger, P., *Proc. Natl. Acad. Sci. USA* **2001,** *98*, 4552-4557.